nagra
National Cooperative for the
Disposal of Radioactive Waste

TECHNICAL REPORT 04-08

A Report of the Spent Fuel Stability (SFS) Project
of the 5th Euratom Framework Program

Estimates of the Instant Release Fraction for UO_2 and MOX Fuel at t = 0

November 2004

L. Johnson, C. Poinssot, C. Ferry and P. Lovera

Hardstrasse 73, CH-5430 Wettingen/Switzerland, Telephone +41-56-437 11 11

nagra
National Cooperative for the
Disposal of Radioactive Waste

TECHNICAL REPORT 04-08

A Report of the Spent Fuel Stability (SFS) Project
of the 5th Euratom Framework Program

Estimates of the Instant Release Fraction for UO_2 and MOX Fuel at t = 0

November 2004

L. Johnson[1], C. Poinssot[2], C. Ferry[2] and P. Lovera[2]

[1] Nagra, Wettingen, Switzerland

[2] CEA, Saclay, France

Hardstrasse 73, CH-5430 Wettingen/Switzerland, Telephone +41-56-437 11 11

This report was prepared on behalf of Nagra. The viewpoints presented and conclusions reached are those of the author(s) and do not necessarily represent those of Nagra.

ISSN 1015-2636

Table of Contents

Table of Contents I
List of Tables II
List of Figures III

1 Introduction 1

2 Overview of radionuclide distribution in fuel assemblies 3

3 Fission gas release from PWR and BWR UO_2 fuel 7

4 Fission gas release behaviour of high burnup fuel and rim restructuring 9

5 MOX fuel – Fission gas release and restructuring 13

6 Leaching of radionuclides from spent fuel and estimated IRF values 17
6.1 Database and representativeness of fuels 17
6.2 Observations based on leaching data 19
6.3 Leachability of grain boundaries 22
6.4 Estimated gap and GB inventories and IRF values for UO_2 fuel 22
6.5 Estimated IRF values for MOX fuel 24

7 Release of radionuclides from fuel assembly structural materials 25
7.1 Concentrations and distributions of radionuclides in Zircaloy cladding 25
7.2 Release rates of radionuclides from Zircaloy cladding 25

8 References 27

List of Tables

Tab. 2-1: Normalised masses of materials used in PWR and BWR fuel assemblies 3

Tab. 2-2: Expected distributions of radionuclides in fuel assemblies and possible modelling approaches 4

Tab. 4-1: Fraction of the total fission gas inventory in a fuel rod that is present in the pores in the rim region of UO_2 fuel with burnups of 37, 41, 48, 60 and 75 GWd/t_{IHM} 12

Tab. 5-1: Microstructural features of AUC MOX (Garcia et al., 2000)..... 15

Tab. 5-2: Microstructural features of ADU MOX (Garcia et al., 2000)..... 15

Tab. 5-3: Distribution of the fission gas in MOX fuel, for various BU (GWd/t_{IHM}); best estimate and pessimistic values..... 15

Tab. 6-1: Gap and grain boundary (GB) leaching data for BWR and PWR fuels 18

Tab. 6-2: Gap and GB inventory estimates (% of total inventory) for various radionuclides for PWR fuel, based on BE values for burnups of 48 GWd/t_{IHM} or less and PE values for higher burnups..... 23

Tab. 6-3: Gap and GB inventory estimates (% of total inventory) for various radionuclides for BWR fuel..... 23

Tab. 6-4: IRF estimates (% of total inventory) for various radionuclides for PWR fuel, assuming IRF comprises gap, GB and all FP in rim region 24

Tab. 6-5: IRF estimates (% of total inventory) for various radionuclides for BWR fuel, assuming IRF comprises gap, GB and all FP in rim region 24

List of Figures

Fig. 3-1: Fission gas release from PWR fuel as a function of burnup (Vesterlund and Corsetti 1994) 7

Fig. 3-2: Fission gas release as a function of burnup for French PWR fuel 8

Fig. 3-3: Fission gas release as a function of average rod burnup (Schrire et al. 1997) 8

Fig. 4-1: Rim width in μm as a function of burnup (GWd/t_{IHM}), from Koo et al. (2001) 10

Fig. 4-2: Fraction of total Xe inventory trapped in rim pores as a function of rim burnup, from Koo et al. (2001) 11

Fig. 5-1: FGR measured in MOX fuels after irradiation and comparison with FGR from UO_2 (Poinssot, unpublished data) 13

Fig. 5-2: Electron micrograph of MOX fuel 14

Fig. 6-1: FGR vs. burnup for UO_2 fuels listed in Tab. 5-1 17

Fig. 6-2: FGR vs. ^{137}Cs gap release measured in leaching experiments, based on data in Tab. 6-1 19

Fig. 6-3: Gap plus grain boundary release of ^{137}Cs vs. FGR (data from Tab. 6-1) 19

Fig. 6-4: Gap plus grain boundary release of ^{129}I vs. FGR (data from Tab. 6-1) 20

1 Introduction

The EU Spent Fuel Stability Project (SFS) aims to develop a **model predicting the radionuclide release rate from spent fuel as a function of time** for geological disposal conditions. Work Package 1 (WP1) of SFS is an important aspect of this model development as it is focused on defining the instant release fraction (IRF), which represents the fraction of the inventory of safety-relevant radionuclides that may be rapidly released from the fuel and fuel assembly materials at the time of canister breaching. The locations of these preferentially released radionuclides, their quantities, the evidence for their release and proposed estimates of the IRF for the key safety-relevant radionuclides[1] for the case of fuel shortly after discharge from the reactor (t = 0) are the subjects of the present report. The potential evolution of the IRF with time in an unbreached canister due to solid-state processes such as diffusion to grain boundaries (alpha self-irradiation enhanced diffusion (αSIED)) or free surfaces has been treated in a separate study (Lovera et al. 2003). These two studies, along with an assessment of the issue of grain boundary stability over time, will ultimately be combined into a comprehensive evaluation of the IRF and combined with the MAM (matrix alteration model) of WP4 in an integrated assessment in WP 5 of the project.

Spent fuel assemblies comprise several materials, including uranium oxide, Zircaloy and various steels or nickel alloys used in the structural components of fuel assemblies. Information on the distribution of both activation products and fission products in all these materials must be taken into account in deriving IRF values. The following sections present information on the radionuclide distributions in the various materials and propose IRF values for key radionuclides. The information in this report is based on the recent study of Johnson and McGinnes (2002), combined with additional data on fission gas release of both UO_2 and MOX fuel, as well as new data on leaching of cesium, all provided by the CEA. The radionuclide concentrations in the various fuel assembly materials are not addressed in the present report.

[1] The selection of safety-relevant radionuclides is normally based on simplified screening models. The nuclides relevant to the IRF considered in this report are based on recent performance assessment studies.

2 Overview of radionuclide distribution in fuel assemblies

Tab. 2-1 gives the normalised masses of the main materials present in typical PWR and BWR assemblies, based on data from McGinnes (2001). The ratios vary somewhat according to fuel assembly design and manufacturer. Notable is the significantly larger mass of Zircaloy per ton of uranium oxide in the case of the smaller BWR fuel assemblies.

Tab. 2-1: Normalised masses of materials used in PWR and BWR fuel assemblies

Fuel assembly type	**Material**	**Mass** [kg]
PWR	UO_2	1000
	Zircaloy-4	267
	Steel	52.3
	Inconel	12.5
BWR	UO_2	1000
	Zircaloy-4	384
	Steel	51.2
	Inconel	4.68

During in-reactor irradiation, radionuclides produced in these materials may stay in the locations in which they are produced or may migrate due to various mechanisms, including recoil, diffusion, grain growth and rim restructuring. An overview of the main fuel assembly components, the nuclides of interest and the expected locations of nuclides upon discharge of the fuel from the reactor is given in Tab. 2-2, based on a number of studies, including Johnson & Tait (1997), Poinssot et al. (2001), Johnson & McGinnes (2002) and Ferry et al. (2004). The degree of segregation of the various radionuclides is highly dependent on fuel operating parameters such as linear power rating and burnup, as discussed in the next section.

Tab. 2-2: Expected distributions of radionuclides in fuel assemblies and possible modelling approaches

Components	Key radionuclides	Characteristics and possible modelling approach
Fuel assembly structural materials		
Zirconia	^{14}C (organic?)	***Oxide film typically about 40 to 80 μm thick is formed in reactor (about 10 % of cladding thickness).The oxide has a low solubility; the outer part is porous and; may incorporate nuclides present in Zircaloy as the film grows.*** Limited data on Zircaloy indicating preferential release; consider ^{14}C as part of IRF. No data on steels.
Zircaloy, Inconel and steel	^{14}C (organic?), ^{36}Cl, ^{59}Ni, ^{63}Ni	Very low general corrosion rate. ***Release of all nuclides plus remaining ^{14}C congruent with the slow corrosion rate***
Uranium oxide fuel		
Gap	Fission gases, volatiles (^{129}I, ^{137}Cs, ^{135}Cs, ^{36}Cl, ^{79}Se, ^{126}Sn(?)). Also ^{14}C (non-volatile but partially segregated)	Good data for some nuclides. Assessment through fission gas release measurements and correlation with leaching experiments. ***Part of IRF***
Rim porosity	Fission gases, volatiles (^{129}I, ^{137}Cs, ^{135}Cs, ^{36}Cl, ^{79}Se, ^{126}Sn(?)) Sr	Rim width a function of burnup; good data available. Large proportion of nuclides in rim region segregated into pores and secondary phases during restructuring. No experimental data indicating release. ***Pessimistically could be part of the IRF; alternatively, may be treated separately (see Section 6.4)***.
Rim grains	Actinides, FP	Release through dissolution when water arrives. FP may also diffuse to rim pores by αSIED. ***FP inventory may thus be part of IRF or MAM.***
Grain boundaries	Fission gases, volatiles (^{129}I, ^{137}Cs, ^{135}Cs, ^{36}Cl, ^{79}Se, ^{126}Sn(?)) Segregated metals (^{99}Tc, ^{107}Pd)	Limited data. ***As for rim pores, pessimistically considered part of IRF, alternatively could be treated separately (see Section 6.4).***
Grains	Actinides, remaining FP and activation products	Belongs to **MAM**, WP4
MOX fuel		
Gap	As for UO_2	Assessment through fission gas release only. Little leaching data. ***Part of IRF.***
Grain boundaries and porosity in PuO_2 grains	As for UO_2	Assessment through fission gas porosity characterisation. ***Conservatively considered part of IRF (see Section 5).***
Grains	As for UO_2	Belongs to **MAM**, WP4

Tab. 2-2 suggests that the definition of what should be included in the IRF is subject to considerable uncertainty and acknowledges subjective assessments regarding likelihood of processes (e.g. leaching of the inventory at the grain boundaries). Recommendations of how to treat these uncertainties will be considered in the final report on the IRF.

As is discussed in Sections 4 and 5, the IRF increases with burnup, paticularly above 50 GWd/t_{IHM}. Ideally, the estimated IRF values as a function of burnup in the present report should be used in conjunction with a histogram giving the numbers of assemblies in various burnup intervals for the spent fuel population in question. This will allow the most realistic estimate of the IRF for the various relevant radionuclides for the entire population of spent fuel for a given repository. Use of bounding FGR values (for example, for high burnup fuel) will lead to overestimates of derived IRF values. Nonetheless, in deriving IRF values, the problem of uncertainties must be given some attention, in particular because there is considerable scatter in FGR data, as well as in data from fission product leaching studies. Furthermore, there are cases where almost no FGR or fission product leaching data are available, thus only more bounding estimates of IRF values based on FGR can be derived. In order to clarify the discussion on the subject of uncertainties, the following approaches and definitions are adopted in this report:

Best estimate (BE) – One based on a good understanding of the mechanism and a good quality database (e.g. FGR in moderate burnup UO_2 fuel and rim restructuring in moderate to high burnup UO_2 fuel).

Bounding or pessimistic estimate (PE) – An estimate based on data and process understanding that provides a maximum for the range of derived values; this is expected to result in significant overprediction of average IRF values. Here this applies particularly to cases where data is extremely limited or unavailable, thus understanding of the processes or of chemical analogues must be used to derive estimates.

In this report, the approach taken is to develop BE IRF values for moderate burnup UO_2 fuel for nuclides for which data exists (^{137}Cs and ^{129}I), because it is judged that the understanding and data are sufficient to support this, and to derive only pessimistic estimate (PE) IRF values for radionuclides for which little data is available and in the case of MOX fuel and higher burnup UO_2 fuel.

3 Fission gas release from PWR and BWR UO_2 fuel

The release of fission gas from UO_2 fuel is strongly correlated with the linear heat rating, which is dependent on fuel temperature (Kamimura 1992). Optimization of fuel assembly designs and irradiation conditions help to ensure that linear heat ratings are kept low and thus FGR is minimized. As a result, FGR values are typically < 1 % at burnups below 40 GWd/t_{IHM}, as shown in Fig. 3-1 for the case of PWR fuel. At higher burnups, a reduction of thermal conductivity increases the fuel temperatures, thus FGR tends to increase (Spino 1998). The results in Fig. 3-1 are consisent with the CEA database for French PWR fuel (Poinssot et al. unpublished data), which extends to ~ 70 GWd/t_{IHM}, as illustrated in Fig. 3-2.

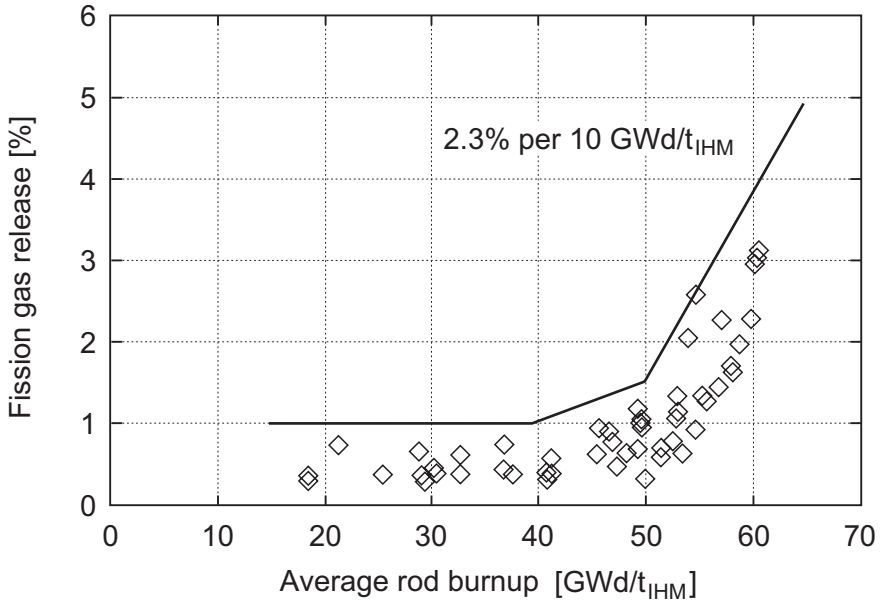

Fig. 3-1: Fission gas release from PWR fuel as a function of burnup (Vesterlund and Corsetti 1994)

The line represents the bounding values of all data.

For BWR fuel, which operates at slightly higher power ratings at high burnups, there is a more pronounced increase in FGR above 45 GWd/t_{IHM}, as seen in the data of Schrire et al. (1997) shown in Fig. 3-3. The results suggest that 5 % is a reasonable best estimate of the average FGR for BWR fuel at a burnup of 45-50 GWd/t_{IHM}. Other data for BWR fuel presented by Hallstadius and Grapengiesser (1990) indicates somewhat higher average gas release at a burnup of 50 GWd/t_{IHM} (up to ~ 10 %). For BWR fuel, there is virtually no published data available for burnups above 50 GWd/t_{IHM}.

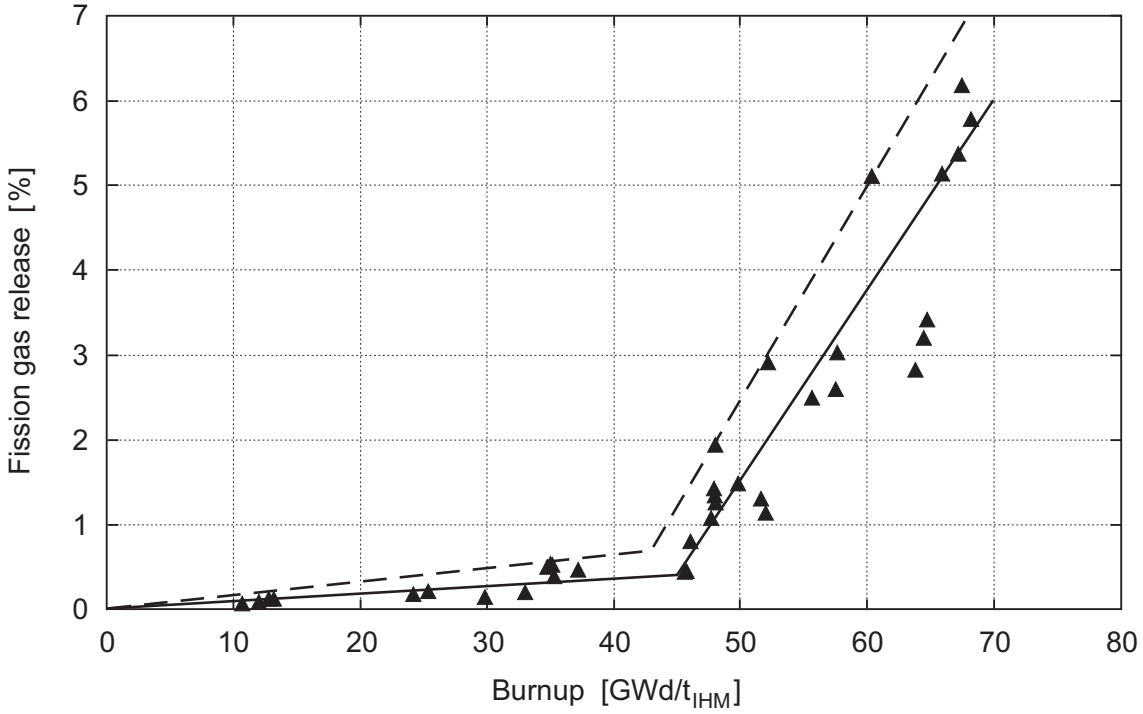

Fig. 3-2: Fission gas release as a function of burnup for French PWR fuel

Solid line – best fit; dashed line – bounding or pessimistic estimate (Poinssot, unpublished data)

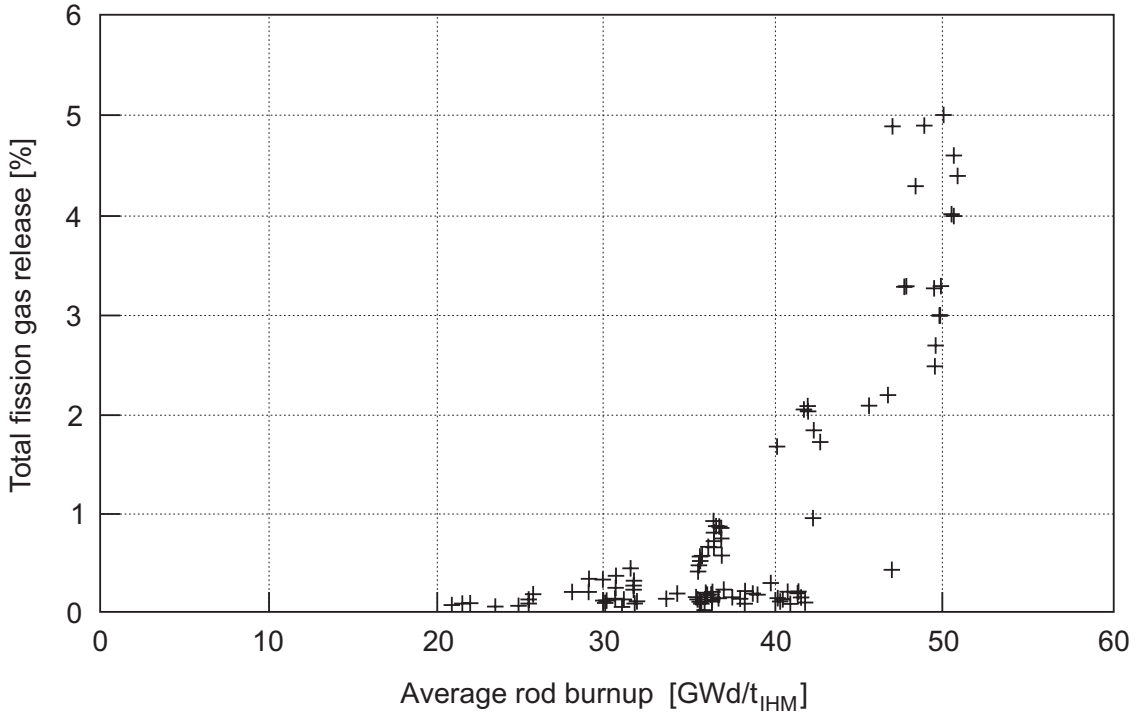

Fig. 3-3: Fission gas release as a function of average rod burnup (Schrire et al. 1997)

There is ample evidence that FGR can be used to give a bounding or pessimistic value for release of most other volatile or semi-volatile nuclides to the gap, as discussed in Section 5.

4 Fission gas release behaviour of high burnup fuel and rim restructuring

Several phenomena occurring in the rim region of fuel pellets result in restructuring of fuel grains. These include:

- high fission density as a result of high yields of ^{239}Pu arising from capture of epithermal neutrons,
- increased porosity,
- reduction in grain size, and
- increased athermal release of fission gas from the grains.

From the perspective of assessing the release of fission products from spent fuel under disposal conditions, the restructuring process may be important, thus it is briefly reviewed here based on studies summarised by Koo et al. (2001). The discussion is based on the assumption of LWR fuel rods with a fuel pellet diameter of ~ 8.2 mm (a 'typical' value).

Fission of ^{239}Pu in the rim region, present at increased concentrations as a result of capture of epithermal neutrons by ^{238}U, leads to a sharp increase in local burnup. Although the outer few μm may reach as much as twice the average pellet burnup, the mean local burnup within the entire rim region is 1.33 times the average pellet burnup. As illustrated in Fig. 4-1, the best estimate of the rim thickness at an average burnup of 50 GWd/t_{IHM} is 50 μm, increasing to 120 μm and 170 μm at 65 and 75 GWd/t_{IHM} using a best fit (Equation 1 in Koo et al. (2001)) of all the data. This best fit is represented by

$$R_t = 3.55BU_R - 185 \quad (1)$$

Where R_t is the rim thickness and BU_R is the rim burnup. Koo et al. (2001) also give a pessimistic function that bounds all the data, given by

$$R_t = 5.28BU_R - 178 \quad (2)$$

However, use of the latter expression suggests that significant rim thicknesses exist even in fuels with burnups in the range of 30 GWd/t_{IHM}. Because this seems completely inconsistent with microstructural studies, a revised expression was developed, given by

$$R_t = 5.44BU_R - 281 \quad (3)$$

This expression gives no rim below 40 GWd/t_{IHM} and is still pessimistic with respect to almost all data points in Fig. 4-1.

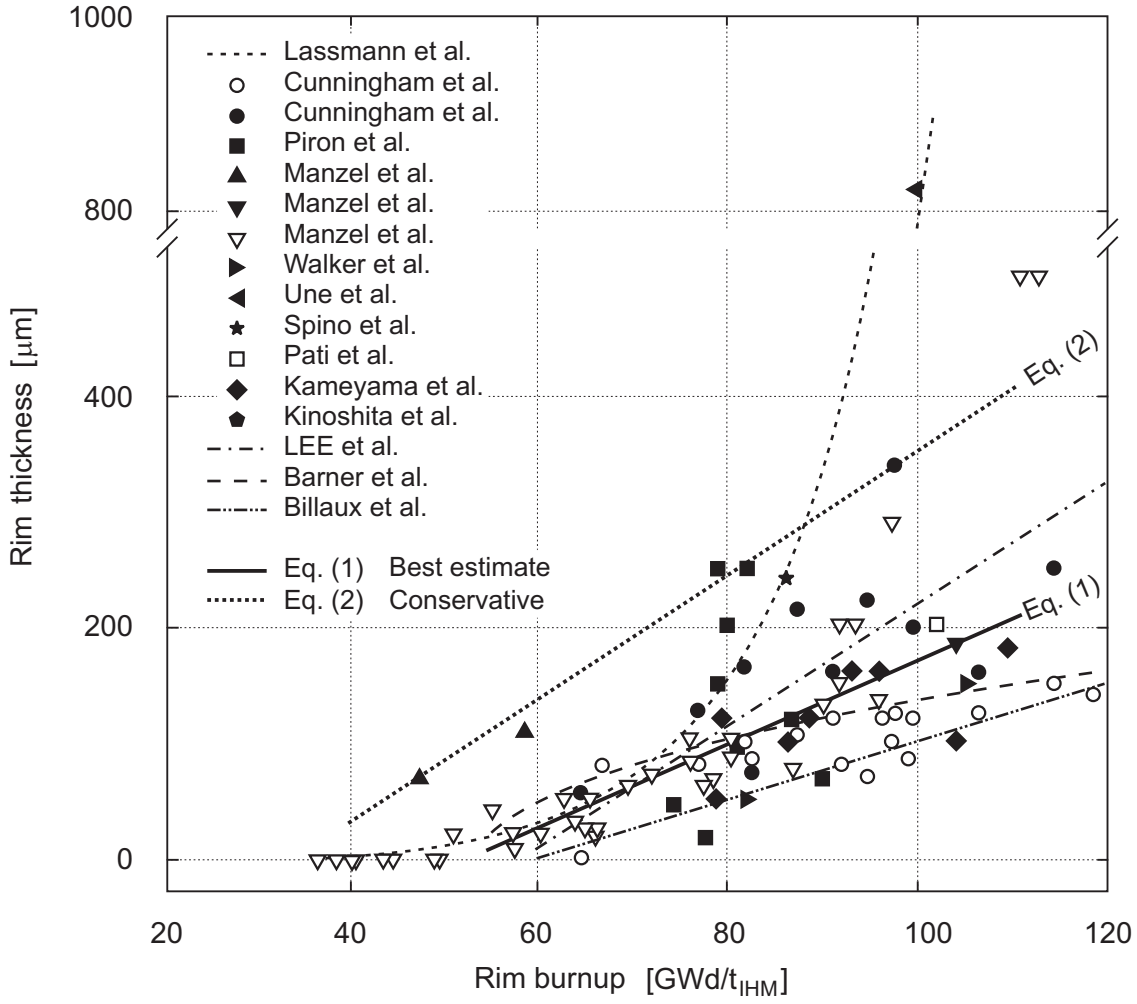

Fig. 4-1: Rim width in μm as a function of burnup (GWd/t_{IHM}), from Koo et al. (2001)

Equation 1 represent a best fit of the data, while Equation 2 is a 'conservative' or pessimistic expression that encompasses almost all the data. The references are in the paper by Koo et al. (2001).

In Koo et al., Equations 1 and 2 are combined with an expression for the Xe distribution in the fuel to calculate the fraction of the total Xe produced in the pellet that is retained in the rim pores assuming no release to the gap during restructuring. This is shown in Fig. 4-2, which illustrates that for a pellet average burnup of 48 GWd/t_{IHM} (rim burnup of 64 GWd/t_{IHM}), the best estimate fraction of Xe trapped in rim pores is ~ 2 %. This increases to 8 % at an average burnup of 75 GWd/t_{IHM} (rim burnup of 100 GWd/t_{IHM}). At high rim burnup, most of the fission gas in the rim is segregated to the pores after rim restructuring (about 85 % at a rim burnup of 80 GWd/t_{IHM}, based on equations in Koo et al. (2001)). As indicated in Fig. 4-1, the scatter in the data used to derive these estimates is large, thus the ‘conservative’ curve proposed by Koo et al. (2001) gives significantly larger rim widths at higher burnups.

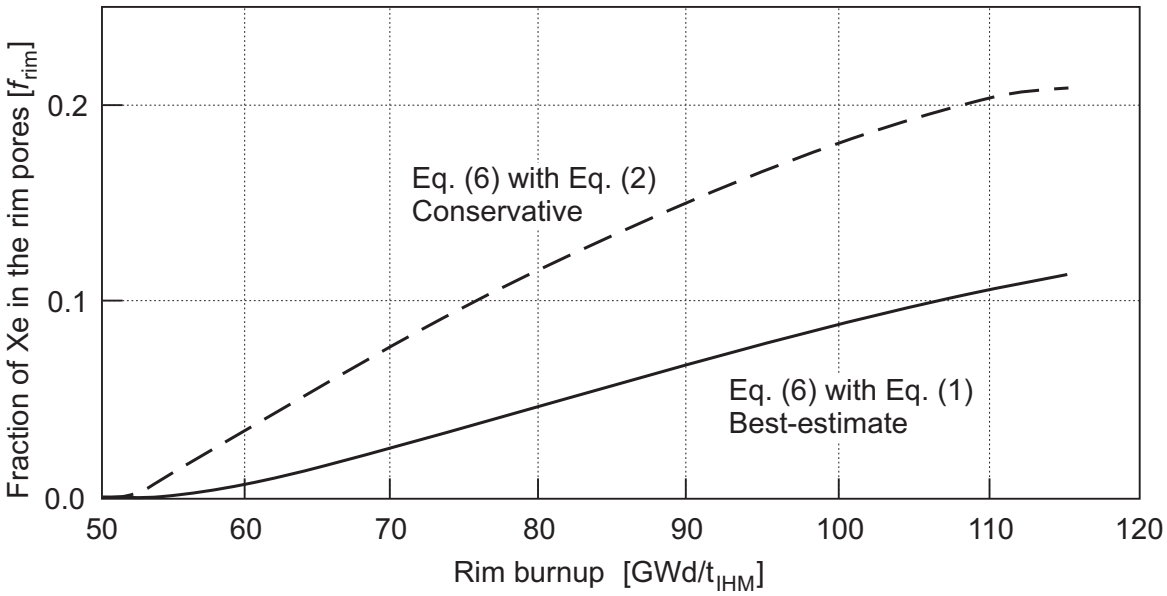

Fig. 4-2: Fraction of total Xe inventory trapped in rim pores as a function of rim burnup, from Koo et al. (2001)

Equations 1, 2 and 6 are given in the original paper.

Within the rim region, the structure is characterised by an average pore size of around 1 μm and an average grain size of 0.5 μm (Poinssot et al. 2001). In spite of the high degree of restructuring, fission gas is typically effectively retained in the new pore structure (Mogensen et al. 1999), which explains the low overall fission gas release for PWR fuels at high burnups (Figs. 3-1 and 3-2). Nonetheless, the fission gas in this region can be considered released from the fuel matrix, even though it is not released to the void space in the fuel rod. Similarly, other fission products that are not in solid solution in UO_2 can be expected to be released from the grains during restructuring. As a result, from the perspective of release under disposal conditions, such fission products can be considered to belong to the grain boundary inventory of the fuel and be potentially available for release if groundwater penetrates grain boundaries.

The fraction of the FG produced that is present in rim pores for various burnups of UO_2 fuel, based on Fig. 4-2 (with revision of the 'conservative' curve according to application of Eq. 3 rather than Eq. 2) is summarised in Tab. 4-1. The total fractional fission gas release from the grains of the fuel to both the free void and closed pores of a fuel element at a given burnup can be considered to be roughly equal to the sum of the measured fission gas releases for the fuel at the given burnup (Figs. 3-1 to 3-3) and the values given in Tab. 4-1. Also given in Tab. 4-1 are the values for the % of total FG inventory in the fuel that is found within the rim region (pores plus grains) based on a simple calculation of the fractional volume of the rim with a correction for the 1.33 times higher average burnup in the rim. This illustrates clearly that most of the fission gas produced in the rim is present in pores (about 70 – 80 %). For the radionuclide release model, options for treating the fission products present within the grains are to consider them as part of the IRF because of the small grain diameter or to consider them being released by matrix dissolution. The question of uncertainties and the impact of using the bounding data in Tab. 4-1 is discussed in Section 5.4.

Tab. 4-1: Fraction of the total fission gas inventory in a fuel rod that is present in the pores in the rim region of UO_2 fuel with burnups of 37, 41, 48, 60 and 75 GWd/t_{IHM}

Values are based on the best estimate (BE) curve in Fig. 4-2 and 'conservative' (pessimistic estimate (PE)) from Eq. 3. The fraction of FG present in the rim region (pores plus grains) is also given.

Average burnup (GWd/t_{IHM})	**Rim burnup** (GWd/t_{IHM})	**% of total FG present in pores in the rim (BE) Eq.1**	**% of total FG present in pores in the rim (PE) Eq.3**	**% of total FG present in the rim (pores + grains) (BE) Eq.1**	**% of total FG present in the rim (pores + grains) (PE) Eq.3**
37	49	0	0	0	0
41	55	0	0.5	0.7	1.25
48	64	2	3	2.7	4.3
60	80	4	8	6.3	9.8
75	100	8	14	10.8	16.5

5 MOX fuel – Fission gas release and restructuring

Fission gas release

The irradiation of MOX fuel on a routine basis in commercial power reactors began in the late 1980s. As a result, compared to FGR data for UO_2 fuels, data for MOX fuel is somewhat limited. The data provided by the CEA (Poinssot, unpublished data) is shown in Fig. 5-1, which shows that FGR for MOX PWR fuel rods increases rapidly above 40 GWd/t_{IHM}. The limited data above 45 GWd/t_{IHM} suggests that the FGR reaches about 5 % at 50 GWd/t_{IHM} and approaches 10 % at 60 GWd/t_{IHM}. Increased FGR relative to UO_2 fuel at higher burnups arises from higher reactivity and higher power/temperatures compared with UO_2 fuel, as well as microstructural factors.

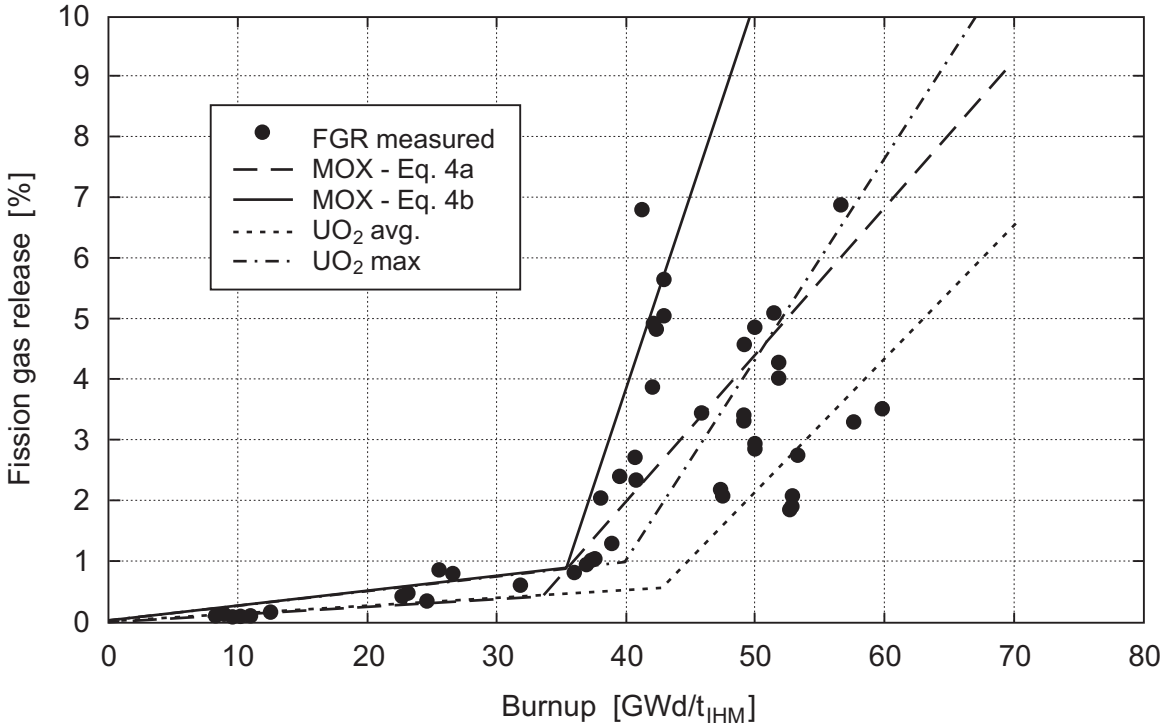

Fig. 5-1: FGR measured in MOX fuels after irradiation and comparison with FGR from UO_2 (Poinssot, unpublished data)

The best estimate or average FGR for MOX fuel in Fig. 5-1 is given by

$$\% \text{ FGR} \approx 0.013 \text{ BU for BU} < \sim 34 \text{ GWd/t}_{IHM} \quad (4a)$$

$$\% \text{ FGR} \approx 0.24 \text{ BU} - 7.6 \text{ for BU} > \sim 34 \text{ GWd/t}_{IHM} \quad (4b$$

The pessimistic FGR is given by

$$\% \text{ FGR} \approx 0.025 \text{ BU for BU} < \sim 35 \text{ GWd/t}_{IHM} \quad (5a)$$

$$\% \text{ FGR} \approx 0.64 \text{ BU} - 21.6 \text{ for BU} > \sim 35 \text{ GWd/t}_{IHM} \quad (5b)$$

Restructuring in MOX fuel

The Pu-rich agglomerates in MOX fuel that have a diameter larger than ~ 10 µm experience a burnup which is much higher than the rest of the fuel, resulting in a structure analogous to that of the rim when they are located in the mid external part of the fuel pellet, as illustrated in Fig. 5-2.

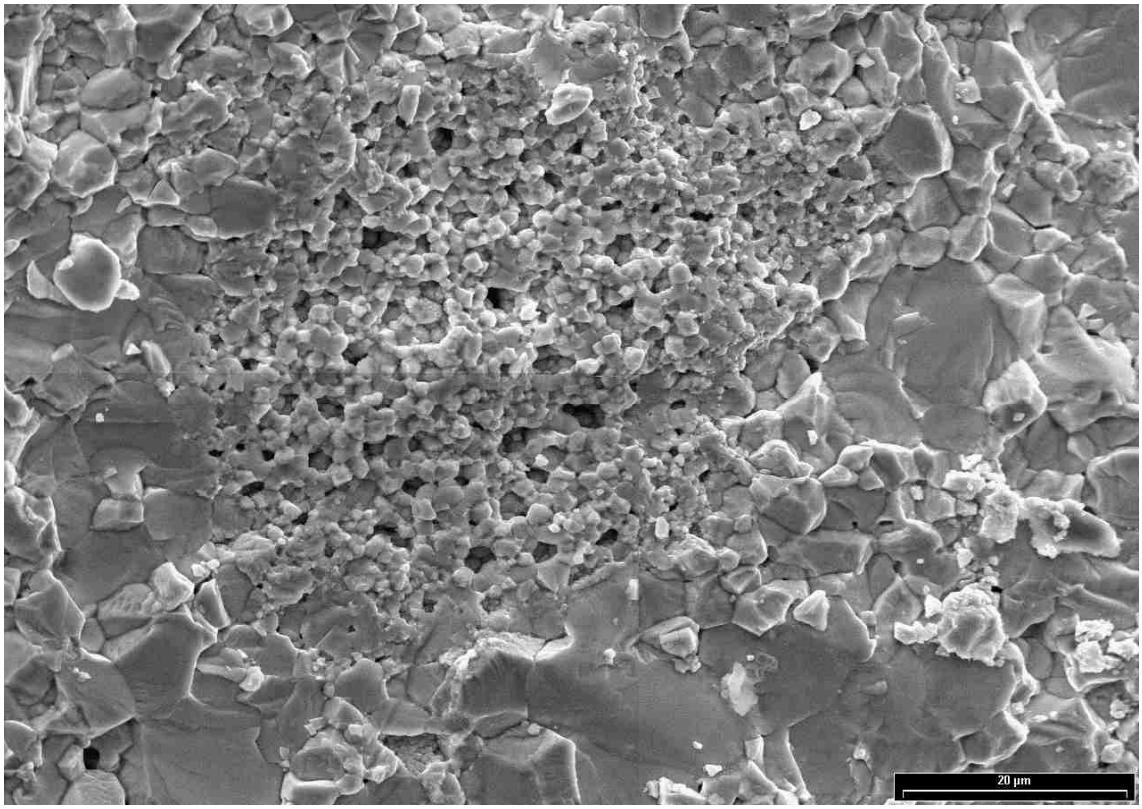

Fig. 5-2: Electron micrograph of MOX fuel

It shows the restructuring and high fission gas porosity in a PuO_2 grain, surrounded by grains of UO_2 with low burnup and little porosity.

Large Pu-rich agglomerates, which represent ~ 11 % of the overall surface, have an average burnup which is ~ 2.5 times higher than the average pellet BU. Thus, fission products present in the large Pu-rich agglomerates represent ~ 25 % of the overall inventory[2]. Moreover, considering the gases undetected by microprobe, Guérin (2002) evaluates the fraction of intergranular gases to be ~ 25 to 30 % in AUC MIMAS fuels with a BU of 45 GWd/t_{IHM} and ~ 30 to 35 % for BU > 50 GWd/t_{IHM}. These values are in agreement with the gas releases observed during experiments of thermal annealing. Most of the gas created is found in aggregate porosity. Thus, the value obtained on the basis of surface distribution of large agglomerates (Tab. 5-1 and 5-2) is in agreement with intergranular gas fraction present essentially in the Pu-rich restructured agglomerates.

[2] proportion of agglomerates in the external zone × surface fraction × average local fission yield

Tab. 5-1: Microstructural features of AUC MOX (Garcia et al., 2000)

	Pu-rich agglomerates	**Phase 'UO_2'**
Surface fraction (%)	24,6[a]	75,4
Plutonium fraction (%)	61,4	38,6
Average Pu concentration % ahm[b]	14,2	2,6

[a] ~ 11 % have a diameter > 20 µm
[b] atoms heavy metal

Tab. 5-2: Microstructural features of ADU MOX (Garcia et al., 2000)

	Pu-rich agglomerates	**Coating phase**	**Phase 'UO_2'**
Surface fraction (%)	11,1	42,2	46,7
Plutonium fraction (%)	38,5	46,3	15,2
Average Pu concentration % ahm[b]	20,2	7,3	2,7

The quantities of fission gas in the gap, the grain boundaries and pores of large Pu rich agglomerates are summarised in Tab. 5-3. A pessimistic estimate is proposed based on the total activity contained in all Pu agglomerates whatever their size (pores plus grains). Assuming an homogeneous distribution of the agglomerates in the pellet, the relative volume of Pu agglomerates in the external zone is ~ 18 % (Poinssot et al. 2001). Taking into account a burnup 3 times higher than that of the matrix, one can infer that the fraction of FP which is present in the Pu agglomerates is ~ 50 % of the total inventory. This evaluation is dependent on the fabrication method, as implied by data in Tab. 5-1 and 5-2.

Tab. 5-3: Distribution of the fission gas in MOX fuel, for various BU (GWd/t_{IHM}); best estimate and pessimistic values

BU(GWd/t_{IHM})		**40**	**45**	**55**	**60**
gap + GB (%)	**average**	2	3,2	5,6	6,8
	pessimistic	3,8	7,0	13,4	16,6
Pu agglomerates (%)	**average**	25	30	30	35
	pessimistic	50	50	50	50
% best estimate		27	33	36	42
% pessimistic estimate		54	57	63	67

The values in Tab. 5-3 are 2-3 times higher than the values proposed in the study of Johnson and McGinnes (2002), which were largely based on gap and grain boundary estimates, without consideration of the release of all fission products contained in the Pu-rich agglomerates. It is clear that, once exposed to water, such porous regions are likely to be susceptible to rapid

leaching of fission products present in the pores. The assumption that the fission product inventory in the agglomerates is part of the IRF is clearly very conservative, as they are not accessible to water when the fuel cladding is breached, because they are surrounded and isolated by grains of dense low porosity UO_2. Nonetheless, in contrast to the question of the leachability of rim porosity and grain boundaries in UO_2, for which there is at least some data to argue that these regions might not be susceptible to leaching, there is little data for MOX fuel. It seems prudent at this stage to use the best estimate and pessimistic estimates in Tab. 5-3 as the basis for the IRF of MOX fuel, at least until the understanding of the leaching behaviour of the material improves.

The relatively limited FGR data for BWR MOX fuel suggests substantially higher releases at 45 to 50 GWd/t_{IHM}, to as much as ~ 25 % (Haas & Lippens 1997). There is no published data on fission gas release from BWR MOX fuel at burnups above 50 GWd/t_{IHM}.

6 Leaching of radionuclides from spent fuel and estimated IRF values

6.1 Database and representativeness of fuels

Although the total number of fuel rods studied to determine the quantities of radionuclides in the gap and at grain boundaries are small, it is nonetheless possible to estimate average values because gap and grain boundary inventories can be correlated with FGR for individual fuel rods and because FGR can be reliably estimated for burnups up to about 50 GWd/t_{IHM} for BWR fuel and 65 GWd/t_{IHM} for PWR fuel. This approach has been used in Canadian (Johnson et al. 1996) and Swedish (Johnson & Tait 1997) assessment studies for CANDU (Canada deuterium uranium) and BWR fuels, respectively.

The relationship between FGR and leaching of a number of fission products from UO_2 fuel has been reviewed recently by Johnson & Tait (1997) and Johnson & McGinnes (2002). In the present study, additional data from the CEA program have been added to the database, as shown in Tab. 6-1. The FGR vs. burnup for all UO_2 fuel in Tab. 6-1 is plotted in Fig. 6-1. It is apparent that the data on FGR from ATM-106 PWR fuel for a burnup of 43-50 GWd/t_{IHM} lie far above the range of values in Figs. 3-1 and 3-2 and above values reported in other studies (e.g., Yokote et al. 1996). The reasons for this are not known (Guenther et al. 1988b), but it is emphasized that review of a large body of FGR data suggests that the result is highly atypical. The data are nonetheless retained in the present study because of the importance of the associated results on fission product leaching.

It should be noted that the data set for leaching of ^{137}Cs, ^{129}I, ^{14}C and ^{36}Cl from CANDU fuel is considerable and is taken into account in estimating IRF values as well, in particular for ^{14}C and ^{36}Cl. A discussion of the CANDU fuel data, which provides much of the basis for the ^{14}C IRF estimates in the present study and provides the only ^{36}Cl leaching data available for spent fuel, is presented in Johnson & Tait (1997). A further important observation is the absence of any leaching data for fuel with burnup exceeding 50 GWd/t_{IHM}. The absence of measurements raises important questions about how to estimate releases for high burnup fuel and how to assess uncertainties. The following discussion summarizes the observations from various leaching studies for each of the relevant radionuclides and presents BE and PE of the IRF for each FP.

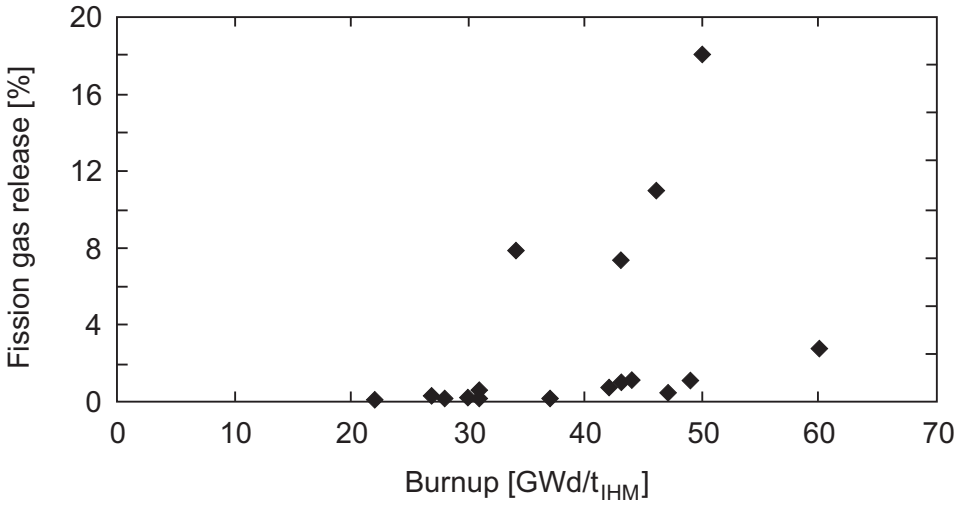

Fig. 6-1: FGR vs. burnup for UO_2 fuels listed in Tab. 5-1

Tab. 6-1: Gap and grain boundary (GB) leaching data for BWR and PWR fuels

Fuel I.D.	Burnup (GWd/t_{IHM})	Fission gas release (%)	Cs Gap (%)	Cs GB (%)	Sr Gap (%)	Sr GB (%)	Tc Gap (%)	Tc GB (%)	I Gap (%)	I GB (%)	C Gap (%)
BWR (Oskarsham) [a]	42	0.7	~ 1								
BWR (Ringhals) [a]	20-49	1.1	0.4-0.8		0.07		0.1 to 0.7				
PWR (Ringhals) [a]	43	1.05	~ 1								
ATM-103 [b] **(PWR)**	30	0.25	0.2	0.48	0.01	0.11					
ATM-104 [b] **(PWR)**	44	1.1	1.2	0.1							
ATM-105 [b] **(BWR)**	31	0.59	0.3	0.1					0.1	2.2	
ATM-105 [b] **(BWR)**	34	7.9	1.5	1.0					2.5	5	
ATM-106 [b] **(PWR)**	43	7.4	2	0.5	0.11	0.03	0.13		0.1	8.5	
ATM-106 [b] **(PWR)**	46	11.0	2.5	1.0	0.02	0.13	0.01	0.01	1.2	8.0	
ATM-106 [b] **(PWR)**	50	18.0	6.5	1.0	0.1	0.07	0.05	0.12	15	7.6	
CEA (PWR) [c]	22	0.1	0.3								
CEA (PWR) [c]	37	0.2	0.6								
CEA (PWR) [c]	47	0.5	2.3								
CEA (PWR) [c]	60	2.8	1.0								
PWR-HBR [d]	31	0.2	0.8		0.024		0.03		0.008		0.001
PWR-TP [d]	27	0.3	0.32		0.012		0.04		0.002		
PWR-HBR [e]	31	0.2							0.284		0.33
PWR-TP [e]	27	0.3	0.4				< 0.01		0.076		3.0
ATM-101 [f] **(PWR)**	28	0.2	2						4		2 to 7
PWR [g]	30	0.36	0.6						0.07		
MOX [h]	12-25	not reported	10 to 12						1 to 2		
MOX [c]	47	7	3.2								

[a] Forsyth & Werme (1992), Forsyth (1997)
[b] Gray (1999); data are estimated from graph as raw data are not presented. Data represent average values of repeat measurements.
[c] Jegou (in preparation)
[d] Oversby & Shaw (1987); Wilson (1988); Data at 25 ° C
[e] Wilson & Shaw (1987); Wilson & Gray (1990); Data at 85 °C
[f] Neal et al. (1988); Crushed fuel, includes grain boundary inventory; Data at 200 °C for 9 months, results likely represent IRF plus some matrix dissolution.
[g] Wegen et al. (2003)
[h] Grambow et al. (2000)

6.2 Observations based on leaching data

Leaching of ^{137}Cs

Gap release of ^{137}Cs vs. FGR for the data in Tab. 6-1 is shown in Fig. 6-2. Notable is that ^{137}Cs gap release is about one third of FGR, except at 1 % FGR, where releases of ^{137}Cs are very similar to FGR.

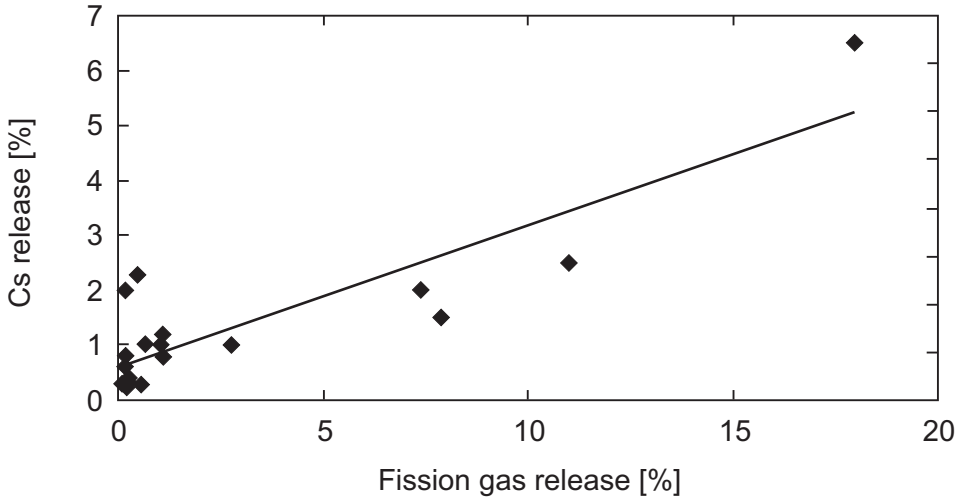

Fig. 6-2: FGR vs. ^{137}Cs gap release measured in leaching experiments, based on data in Tab. 6-1

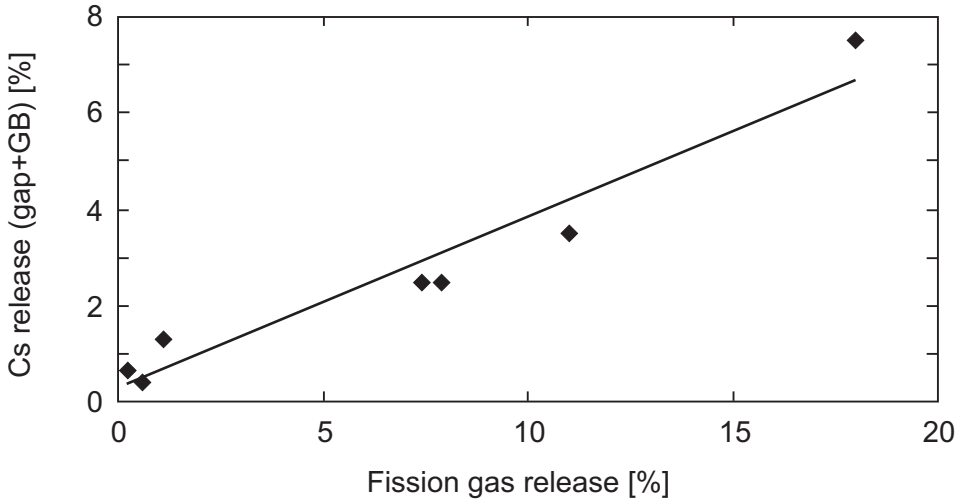

Fig. 6-3: Gap plus grain boundary release of ^{137}Cs vs. FGR (data from Tab. 6-1)

Gray (1999) measured both gap and grain boundary inventory values of ^{137}Cs for several PWR and BWR fuels. In all cases, the release from grain boundaries was ~ 1 % or less. A plot of the sum of gap and grain boundary inventories again yields a correlation for ^{137}Cs: FGR of ~ 1:3 (Fig. 6-3). Grain boundary inventories of ^{137}Cs are relatively small, even for high FGR fuels. Such a result is consistent with the finding that the diffusion coefficient of Cs in UO_2 is lower than that of fission gases (Poinssot et al. 2001). Studies of high linear power CANDU fuel by

Stroes-Gascoyne et al.(1993) also indicate that grain boundary inventories are smaller than gap inventories. The results of Forsyth (1997), showed that ^{137}Cs release from clad fuel rod sections increased with burnup from 0.5 % to 1 % in the interval from 25 to 43 GWd/t_{IHM}, decreasing slightly in the interval of 43 to 49 GWd/t_{IHM}. This may be associated with the closure of the fuel/clad gap that is observed as burnup increases (Poinssot et al. 2001), thus the finding does not necessarily contradict the general observation of increased fission gas and IRF with increased burnup.

Leaching of ^{129}I

Gray (1999) suggested that there is a ~ 1:1 correlation between the sum of gap and grain boundary releases and FGR. This result appears consistent with the observation that the diffusion coefficients of I and fission gases may be similar (Poinssot et al. 2001). However, the majority of the fraction of ^{129}I released from the matrix resides in grain boundaries, not in the gap (Tab. 6-1), in contrast to the behaviour of ^{137}Cs. A linear regression of all the ^{129}I data (gap plus grain boundary vs. FGR) in Tab. 5-1, including the data of Neal et al. (1988), which is for crushed fuel, yields a slope of 1 and a best estimate release value of 6.5 % at 5 % FGR, as shown in Fig. 6-4. Included in Fig. 6-4 is a pessimistic estimate line that encompasses all the data.

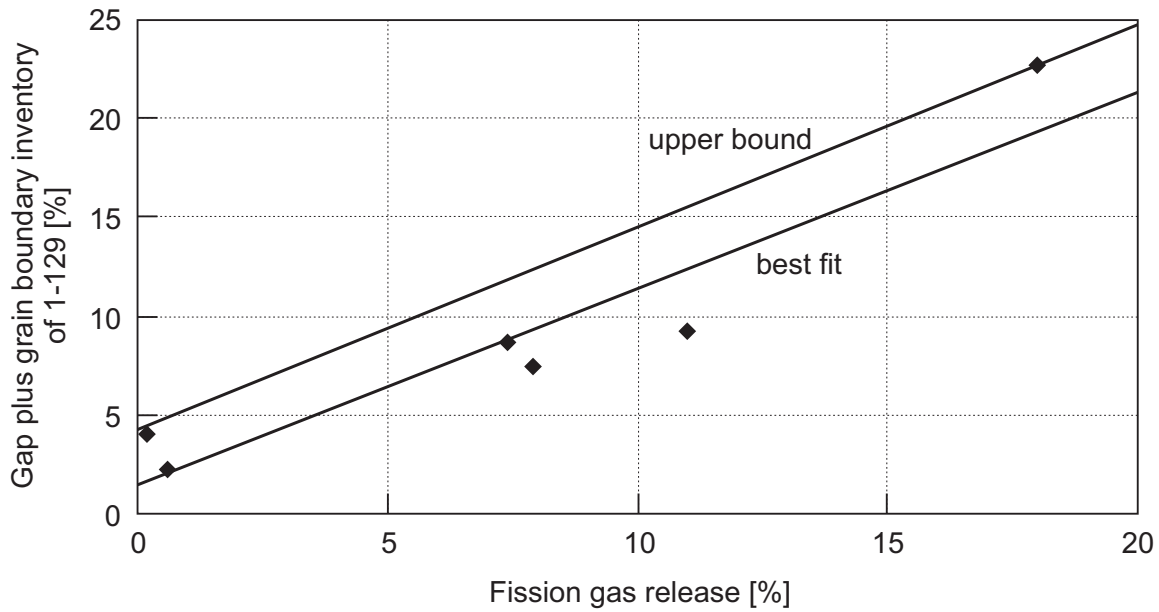

Fig. 6-4: Gap plus grain boundary release of ^{129}I vs. FGR (data from Tab. 6-1)

Leaching of ^{36}Cl

As noted by Johnson & Tait (1997), there is no data on leaching of ^{36}Cl from LWR fuels. The estimated IRF is thus based on the CANDU fuel data of Tait et al. (1997), which shows that ^{36}Cl releases increase sharply with FGR, reaching values three times the FGR for high linear power rating fuels. It should be noted that the linear power rating of CANDU fuel is much higher than that of LWR fuel, thus use of this data for LWR fuel is likely to overestimate releases. Only bounding IRF values for ^{36}Cl can be estimated, acknowledging the absence of data for LWR fuel.

Leaching of ^{14}C

No new data for ^{14}C has been reported since the review of Johnson & Tait (1997). It should be noted that the sparse data for LWR fuel in Tab. 6-1 are in good agreement with the data for CANDU fuel, for which Stroes-Gascoyne et al. (1994) report an average IRF of 2.7 % based on a large number of measurements. The latter study noted that the IRF of ^{14}C is independent of fuel power rating, thus the CANDU fuel data appear to be directly applicable to the case of the lower rating LWR fuel. The chemical form of released ^{14}C is unknown, because studies of release of ^{14}C from spent fuel normally involve oxidative treatment of the solution to capture $^{14}CO_2$ for chemical analysis (Stroes-Gascoyne et al. 1994). Again it appears prudent to define only a pessimistic value for the IRF of ^{14}C, given the paucity of measurements.

Leaching of ^{79}Se and ^{126}Sn

Wilson (1987, 1990) attempted to measure release of both ^{79}Se and ^{126}Sn in his experiments performed for the Yucca Mountain Project. Data for the nuclides ^{137}Cs, ^{90}Sr, ^{99}Tc, ^{129}I and ^{14}C from these experiments is included in Tab. 2-2. None of the measurements of ^{79}Se in solution yielded detectable concentrations. Nonetheless, from the 'less than' data reported in his tables, it is possible to infer a maximum IRF value. For the H.B. Robinson fuel, an IRF value of < 0.025 % is obtained, after correction of the inventory value (required because of the revision in the half-life to 1.1×10^6 a) using the data from Guenther et al. (1988a). This calculated IRF is significantly lower than FGR of 0.2 %, raising questions about the conservative assumption that Se is in the volatile group. Gap release values that are $1/10^{th}$ of the FGR are thus assumed. For ^{126}Sn, less than values are also reported; however, in this case, releases of < 0.005 % can be derived. This suggests that there is no real evidence for segregation at low burnup. Accordingly, ^{126}Sn is assigned a gap release of 0.01 %. Both nuclides are retained in the group of nuclides with a significant GB release at higher burnup, based on the assumption that they are incompatible with the lattice during grain restructuring in the rim.

Release of other radionuclides

A number of other radionuclides need to be considered in the safety assessment with respect to their potential to segregate from UO_2 during reactor irradiation and be released preferentially into groundwater. These include[3] ^{14}C, ^{36}Cl, ^{90}Sr, ^{99}Tc and ^{107}Pd. The approach to estimating IRF values for other radionuclides is discussed in Johnson & Tait (1997).

For many of the radionuclides for which leaching measurements are not available, the only basis for the estimates are the observations that diffusion coefficients in UO_2 during reactor irradiation decrease in the order FG $\approx$ I > Cs > other fission products, and the understanding of fission product chemistry, which has identified which fission products form solid solutions with UO_2 and which form secondary phases (Johnson & Shoesmith 1988). An indication that using Cs or I to bound the release of other fission products is a conservative approach can be obtained by considering the case of Cd, one of the most volatile of the fission products (after FG, Cs and I) (Cubicciotti & Sanecki 1978). Quantitative X-ray photoelectron spectroscopy of grain boundaries in CANDU fuel has been performed by Hocking et al. (1994), who noted that Cd was only occasionally detected and would have been routinely seen if it had experienced the same fractional release as Cs. Iodine was not observed perhaps because of its low fission yield. The IRF for ^{129}I should thus provide a bounding value which would not be exceeded by other fission products. There is some doubt whether Pd and Tc should be included in the category of nuclides with a significant IRF, as these elements are present in UO_2 as insoluble alloy

[3] This list of nuclides may vary depending on requirements of the safety assessment in question.

inclusions, thus releases are extremely small, as noted in leaching studies (see Tab. 5-1). Nonetheless, because they segregate significantly to grain boundaries, values are assigned here based on the extent of restructuring in the rim region.

6.3 Leachability of grain boundaries

An issue of considerable difficulty in assessing long-term behaviour of spent fuel is the question of leachability and long-term stability of grain boundaries. It is clear that grain boundaries in spent fuel are regions of high local accumulations of fission gas and solid fission products. In particular, the presence of large numbers of fission gas bubbles and some soluble fission products has led to speculation that selective dissolution might occur and that water might percolate along grain boundaries, gradually leaching out fission products as well as increasing the surface area of the fuel. Since the early days of spent fuel studies, the gap and grain boundary inventories have both been considered to contribute to the IRF (Johnson et al. 1985). The reasons for this relate to the difficulties in assessing grain boundary penetration in dissolution experiments coupled with the desire to develop a 'conservative' model for fuel dissolution to satisfy performance assessment requirements. The evidence regarding leachability of grain boundaries remains contradictory and has not been further evaluated in the SFS Project.

6.4 Estimated gap and GB inventories and IRF values for UO_2 fuel

The estimated gap and grain boundary inventories for important radionuclides are listed in Tab. 6-2 and 6-3 for PWR and BWR UO_2 fuels with burnups of 37, 41, 48, 60 and 75 GWd/t_{IHM}. All other radionuclides are assumed to be homogeneously distributed in the fuel matrix. The approach in developing the estimates has been to use best estimate (BE) correlations of Cs and I release with FGR to estimate the gap values for all burnups. GB inventories for Cs and I are based on BE values up to 48 GWd/t_{IHM}, including the rim porosity values in Tab. 4-1. Rather pessimistic values for ^{14}C and ^{36}Cl are adopted because of the very limited data and understanding of release behaviour for these nuclides. For higher burnups, the fission gas release is used to bound the gap release of volatile and semi-volatile radionuclides. The GB releases at high burnups are based on the pessimistic estimate values for rim porosity in Tab. 4-1, combined with smaller GB contributions for the rest of the fuel. The approach is somewhat different from that in Johnson & McGinnes (2002), in that gap and grain boundary estimates are explicitly identified here to permit options for treating their release, i.e., to consider IRF to be equal to gap inventories only or gap plus grain boundary inventories.

An optional approach is to assume pessimistically that water penetrates all pores rapidly and alpha self-irradiation-enhanced diffusion of fission products occurs. The latter process would effectively lead to rapid release of all FP in the rim region, because of the small grain size. This leads to the IRF values in Tab. 6-4 and 6-5.

Tab. 6-2: Gap and GB inventory estimates (% of total inventory) for various radionuclides for PWR fuel, based on BE values for burnups of 48 GWd/t_{IHM} or less and PE values for higher burnups

BURNUP	**37**		**41**		**48**		**60**		**75**	
RN	Gap	GB	Gap	GB	Gap	GB	Gap	GB	Gap	GB
fission gas	1	1	1	1	1	3	4	8	8	14
^{14}C	10		10		10		10		10	
^{36}Cl	5		5		10		12		25	
^{79}Se	0.1	1	0.1	1	0.1	2	0.4	8	0.8	14
^{90}Sr	1	-	1	-	1	-	1	8	1	14
^{99}Tc	0	1	0	1	0	2	0	8	0	14
^{107}Pd	0	1	0	1	0	2	0	8	0	14
^{126}Sn	0.01	1	0.01	1	0.01	2	0.01	8	0.01	14
^{129}I	1	2	1	2	1	3	4	8	8	14
^{135}Cs	1	1	1	1	1.5	1	4	8	8	14
^{137}Cs	1	1	1	1	1.5	1	4	8	8	14

Tab. 6-3: Gap and GB inventory estimates (% of total inventory) for various radionuclides for BWR fuel

BURNUP	**37**		**41**		**48**	
RN	Gap	GB	Gap	GB	Gap	GB
fission gas	1	1	1	1	5	3
^{14}C	10	10	10	10	10	10
^{36}Cl	5		5		13	
^{79}Se	0.1	1	0.1	1	0.5	2
^{90}Sr	1	1	1	1	1	1
^{99}Tc	0	1	0	1	0	2
^{107}Pd	0	1	0	1	0	2
^{126}Sn	0.01	1	0.01	1	0.01	2
^{129}I	1	2	1	2	5	4
^{135}Cs	1	1	1	1	2	3
^{137}Cs	1	1	1	1	2	3

Tab. 6-4: IRF estimates (% of total inventory) for various radionuclides for PWR fuel, assuming IRF comprises gap, GB and all FP in rim region (grains plus pores)

BE values, with PE values in brackets

BURNUP	**37**	**41**	**48**	**60**	**75**
RN	IRF	IRF	IRF	IRF	IRF
fission gas	2 (2)	2 (3)	4 (6)	10 (16)	18 (26)
^{14}C	10	10	10	10	10
^{36}Cl	5	5	10	16	26
^{79}Se	1 (1)	1 (1)	3 (4)	7 (11)	11 (17)
^{90}Sr	1 (1)	1 (2)	3 (4)	7 (11)	11 (17)
^{99}Tc	1 (1)	1 (2)	3 (4)	7 (11)	11 (17)
^{107}Pd	1 (1)	1 (2)	3 (4)	7 (11)	11 (17)
^{126}Sn	1 (1)	1 (2)	3 (4)	7 (11)	11 (17)
^{129}I	3 (3)	3 (3)	4 (6)	10 (16)	18 (26)
^{135}Cs	2 (2)	2 (2)	4 (6)	10 (16)	18 (26)
^{137}Cs	2 (2)	2 (2)	4 (6)	10 (16)	18 (26)

Tab. 6-5: IRF estimates (% of total inventory) for various radionuclides for BWR fuel, assuming IRF comprises gap, GB and all FP in rim region (grains plus pores)

BE values, with PE values in brackets

BURNUP	**37**	**41**	**48**
RN	IRF	IRF	IRF
fission gas	2 (3)	2 (3)	8 (10)
^{14}C	10	10	10
^{36}Cl	5	5	13
^{79}Se	1 (1)	1 (2)	3 (4)
^{90}Sr	1 (1)	1 (2)	3 (6)
^{99}Tc	1 (1)	1 (2)	3 (4)
^{107}Pd	1 (1)	1 (2)	3 (4)
^{126}Sn	1 (1)	1 (2)	3 (4)
^{129}I	3 (3)	3 (3)	8 (10)
^{135}Cs	2 (2)	2 (3)	6 (8)
^{137}Cs	2 (2)	2 (3)	6 (8)

6.5 Estimated IRF values for MOX fuel

The values presented in Tab. 5-3 for FG segregation in MOX fuel are proposed as IRF values, for the reasons discussed in Section 5.

7 Release of radionuclides from fuel assembly structural materials

7.1 Concentrations and distributions of radionuclides in Zircaloy cladding

A variety of radionuclides are present in the Zircaloy cladding and other structural materials in LWR fuel elements. These radionuclides are produced by neutron activation of alloying elements and impurities present in the as-fabricated materials. The most important of these in terms of long-term safety assessment are ^{14}C, ^{36}Cl, ^{59}Ni and ^{63}Ni.

Because the impurities in Zircaloy are uniformly distributed, and the temperature of the cladding during in-reactor irradiation and the associated solid-state diffusion rates are relatively low, the activation products would be expected to be likewise uniformly distributed on a microscopic scale (although there will be larger-scale variations because of flux variation within fuel rods). There is, however, evidence that ^{14}C has a higher concentration in the oxide film than in the underlying alloy. For example, Yamaguchi et al. (1999) determined that 17 % of the ^{14}C in cladding is present in the oxide film. Assuming that the oxide film in their study was about 60 µm thick, this represents a ^{14}C concentration in the oxide film that is at least three to four times that in the underlying alloy. A similar ^{14}C enrichment in the oxide film was observed by Smith & Baldwin (1993). For other long-lived radionuclides present at trace levels in Zircaloy, eg., ^{36}Cl, ^{59}Ni and ^{63}Ni, the distributions within cladding are unknown, although within the alloy itself they are likely to be present as grain-boundary phases.

7.2 Release rates of radionuclides from Zircaloy cladding

The release of radionuclides from cladding is expected to be controlled in large part by the uniform corrosion rate of Zircaloy (the case of ^{14}C is discussed further below). At the low temperatures in a repository, the data are rather limited, but the study of Rothman (1984) has dealt with the question of extrapolation of high-temperature (in-reactor) uniform corrosion rates down to 150 °C. At this temperature, he estimated that the rate would be ~ 1 nm a^{-1}, and signify-cantly lower rates would be expected at lower temperatures as the repository cools. Rothman also notes that the corrosion rate is expected to be the same in low salinity groundwaters. A study of the corrosion rate of irradiated Zircaloy pressure tube material at 90 °C in aerated Hanford River water by Johnson (1977) gave an estimated rate of 3 to 5 nm a^{-1}. Videm (1981) reported corrosion rates for unirradiated Zircaloy of 0.1 to 1 nm a^{-1} in aerated KBS groundwater at 85 °C. It is also worth noting that the uniform corrosion rate of a similar metal, titanium, is reported to be ~ 2 nm a^{-1} in water-saturated bentonite at 90 °C (Mattsson & Olefjord (1984, 1990) and Mattsson et al. (1990)). For materials such as titanium and zirconium alloys, the very thin passive oxide film is produced as a result of oxidation by water, thus the presence of oxygen in solution is not required for the maintenance of passivity. Based on the above values, and giving particular weight to the rates reported by Johnson (1977) for irradiated material, a maximum corrosion rate of 10 nm a^{-1} is proposed for spent fuel cladding for radionuclides entrained in the Zircaloy.

Two other recent studies report the corrosion rate of unirradiated Zircaloy, measured using H_2 evolution methods in alkaline pore water (pH 10 to 13.5) at temperatures of 30 to 50 °C. These data are particularly relevant to the conditions in a low and intermediate level waste repository. Wada et al. (1999) reported initial corrosion rates of 1 nm a^{-1}, dropping to ~ 0.1 nm a^{-1} after 300 days. The highest long-term rate (0.3 nm a^{-1}) was observed at pH 10 and 50 °C. At pH 13.5 and 30 °C the rate was similar to that at pH values of 10 and 12.5. Kurashige et al. (1999) measured the H_2 evolution rate of Zircaloy in alkaline pore water at 30 and 45 °C. They reported

average rates of 1 to 2 nm a^{-1} after 400 to 500 days. Some samples were treated with steam at 400 °C to thicken the oxide film, but this had no effect on the subsequent low temperature corrosion rate. Yamaguchi et al. (1999) observed that a corrosion rate of 0.03 μm a^{-1} appeared to account for the ^{14}C release from a cladding sample with the oxide film removed. The difference between their rate and the lower rate extrapolated from high temperature studies may be a result of an acceleration in the corrosion rate caused by removal of the protective oxide film. Besides the difficulty of estimating an appropriate long-term corrosion rate of the alloy, there remains the observation of a rather high concentration of ^{14}C in the oxide film (Yamaguchi et al. (1999)), the release of which occurred at a rate considerably greater than that from the alloy itself. Van Konynenburg et al. (1987) and Smith & Baldwin (1993) also reported a rapid release of ^{14}C (< 1 % of the total inventory) in air oxidation and water corrosion studies on Zircaloy cladding. For the present study, the release of ^{14}C from the oxide film is assumed to be rapid, and is represented as an IRF for the cladding of 20 %. The remaining ^{14}C is assumed to be released congruently with the uniform corrosion of the Zircaloy, at a corrosion rate of 0.01 μm a^{-1}. Assuming that corrosion occurs from both sides of the cladding and the cladding thickness is ~ 600 μm, radionuclide release would occur at a constant rate of $\sim 3 \times 10^{-5}$ a^{-1} of the initial inventory.

The corrosion rate in saturated NaCl brines may be significantly higher, as indicated by measurements discussed in Grambow et al. (2000), where values in the range of 0.1 to 0.4 μm a^{-1} were reported. In this case, complete corrosion of Zircaloy and release of activation products might occur over as short a time as ~ 1000 years.

An additional special consideration for release calculations for ^{14}C is its chemical form. It is likely that ^{14}C is present in cladding as carbide. Studies of the corrosion of steel containing carbides in anoxic water indicate that a range of range of hydrocarbons are produced, including methane, ethene, ethane, propane, propene and butenes (Deng et al. 1997). In the case of leaching in anoxic cement pore water, Yamaguchi et al. (1999) observed that ^{14}C was released in organic form, although they detected it in the aqueous phase only. Nonetheless, under the high hydrogen partial pressure conditions expected in the repository, the ^{14}C may be converted to a form such as methane. As a result, radionuclide transport scenarios should consider the possibility of gas phase transport of ^{14}C from the near field.

8 References

Cubbicciotti, D. & J.E. Sanecki. 1978. Characterization of deposits on inside surfaces of LWR cladding. J. Nucl. Mater. 78 ,96-111.

Deng, B., T.J. Campbell & D.R. Burris. 1997: Hydrocarbon formation in metallic iron/water systems. Environ. Sci. Technol. 31, 1185-1190.

Ferry, C., P. Lovera, C. Poinssot & L.H. Johnson. (2004). Quantitative assessment of the instant release fraction (IRF) for fission gases and volatile elements as a function of burnup and time under geological disposal conditions, Scientific Basis for Nuclear Waste Management XXVII, Kalmar, June 2003, Vol. 807, pp. 35-40, MRS.

Forsyth, R.S. & L.O. Werme. 1992: Spent fuel corrosion and dissolution. J. Nucl. Mater. 190, 3-19.

Forsyth, R.S. 1997. The SKB Spent Fuel Corrosion Programme. An evaluation of results from the experimental programme performed in the Studsvik Hot Cell Laboratory. SKB Technical Report 97-25.

Garcia, Ph, Bouloré, A., Guérin, Y., Trotabas, M., Goeuriot, P. 2000. In-pile densification of MOX fuels in relation to their initial microstructure. ANS 2000, Park City

Gates, G.A., P.M.A. Cook, P. De Klerk, P. Morris, & I.D. Palmer. 1998: Thermal Performance Modelling with the ENIGMA Code, in Thermal Performance of High Burn-Up LWR Fuel, Seminar Proceedings, Cadarache, 3-6 March, 1998, OECD/NEA, Paris.

Grambow, B.,A. Loida, A. Martinez-Esparza, P. Diaz-Arocas, J. De Pablo, J.-L. Paul, G. Marx, J.-P. Glatz, K. Lemmens, K. Ollila & H. Christensen. 2000: Source term for peformance assessment of spent fuel as a waste form. European Commission Report EUR 19140 EN.

Gray, W.J., L.E. Thomas & R. Einziger 1993. Effects of air oxidation on the dissolution rate of LWR spent fuel. Mat.Res. Soc. Symp. Proc. Vol. 294, pp. 47-54. Materials Research Society, Pittsburgh.

Gray, W. J., & L.E. Thomas. 1994. Initial results from dissolution testing of various air-oxidized spent fuels. Mat.Res. Soc. Symp. Proc. Vol. 333, pp. 391-398. Materials Research Society, Pittsburgh.

Gray, W.J. 1999: Inventories of I-129 and Cs-137 in the gaps and grain boundaries of LWR spent fuels. In Scientific Basis for Nuclear Waste Management XXII, (D. J. Wronkewiecz and J.H. Lee, Editors), Mat. Res. Soc. Symp. Proc. Vol. 556, 487-494, MRS, Pittsburgh, Pennsylvania.

Gray, W.J. & D.M. Strachan. 1991: UO_2 matrix dissolution rates and grain boundary inventories of Cs, Sr and Tc in spent LWR fuel, Mat.Res. Soc. Proc. Vol. 212, pp 205-212, Materials Research Society, Pittsburgh.

Guenther, R.J., D. E. Blahnik, T.K. Campbell, U.P. Jenquin, J.E. Mendel, L.E. Thomas & C. K. Thornhill. 1988a: Characterization of spent fuel approved testing material ATM-103, Pacific Northwest Laboratory Report PNL-5109-103.

Guenther, R.J., D. E. Blahnik, T.K. Campbell, U.P. Jenquin, J.E. Mendel, & C. K. Thornhill. 1988b: Characterization of spent fuel approved testing material ATM-106, Pacific Northwest Laboratory Report PNL-5109-106.

Guerin, Y., D. Lespiaux, C. Struzik & L. Caillot. 1999. Behaviour of MOX fuel as compared to UO_2 fuel. Physics and Fuel Performance of Reactor-Based Plutonium Disposition, Workshop Proceedings, Paris, 28-30 September 1998. NEA Paris.

Haas, D. & M. Lippens. 1997: MOX fuel fabrication and in-reactor performance. Proceedings Global '97, Oct. 5-19, 1997, Yokohama, pp. 489-494.

Hallstadius, L. & B. Grapengiesser. 1990: Progress in understanding high burnup phenomena. Proc. IAEA Technical Committee Meeting on Fuel Performance at High Burnup for Water Reactors. Studsvik 1990. IAEA, IWGFPT-36, 52-57.

Hocking, W.H., A.M. Duclos And L.H. Johnson. 1994. Study of fission-product segregation in used CANDU fuel by X-ray photoelectron spectroscopy (XPS) II, J. Nucl. Mat. 209, 1-26.

Jegou, C., unpublished data.

Johnson, A.B. 1977: Behavior of spent nuclear fuel in water pool storage, Pacific Northwest Laboratory Report, BNWL-2256, Richland, Washington.

Johnson, L.H., Garisto, N.C., Stroes Gascoyne, S., "Used Fuel Dissolution Studies in Canada", in Proc. Waste Management 1985, (eds., R.G. Post, M.E. Wacks), p. 479 (1985).

Johnson, L.H., D.M. Leneveu, F. King, D.W. Shoesmith, M. Kolar, D.W Oscarson, S. Sunder, C. Onofrei, & J.L. Crosthwaite. 1996: The disposal of Canada's nuclear fuel waste: a study of postclosure safety of in-room emplacement of used CANDU fuel in copper canisters in permeable plutonic rock. Volume 2: Vault model. Atomic Energy of Canada Limited Report AECL-11494-2, COG-95-552-2.

Johnson, L.H. & D.W. Shoesmith 1988: Spent Fuel, in Radioactive Waste Forms for the Future, eds. W. Lutze and R.C. Ewing, Elsevier Science Publishers.

Johnson, L.H. & J.C. Tait. 1997: Release of Segregated Radionuclides from Spent Fuel, SKB Technical Report 97-18.

Johnson, L.H. & D.F. McGinnes. 2002: Partitioning of radionuclides in Swiss power reactor fuels. Nagra Technical Report NTB 02-07.

Kamimura, K. 1992: FP gas release behavour of high burnup MOX fuels for thermal reactors, Proc. of Technical Committee Meeting on Fission Gas Release and Fuel Rod Chemistry Related to Extended Burnup, Pembroke, Ontario, Canada, 28 April-1 May 1992, IAEA-TECDOC-697, p. 82.

Koo, Y.-H., Lee, B.-H., Cheon, J.-S. & Sohn, D.-S. 2001: Pore pressure and swelling in the rim region of LWR high burnup UO_2 fuel. J. Nucl. Materials 295, pp. 213-230.

Kurashige, T., R. Fujisawa, Y. Inagaki & M. Senoo. 1999. Gas generation behavior of Zircaloy-4 under waste disposal conditions, in Radioactive Waste Management and Environmental Remediation, In ICEM Conference Proceedings, Nagoya, Japan, Sept. 26-30, 1999, ASME.

Lovera, P., C.Ferry, C. Poinssot & L. Johnson. 2003: Synthesis report on the relevant diffusion coefficients of fission products and helium in spent nuclear fuels. Commisariat l'Énergie Atomique report CEA-R-6039.

Mattsson, H. & I. Olefjord. 1984: General corrosion of Ti in hot water and water saturated bentonite clay. Swedish Nuclear Fuel and Waste Management Company Report, SKB-KBS-TR-84-19.

Mattsson, H. & I. Olefjord. 1990: Analysis of oxide formed on titanium during exposure in bentonite clay. I. The oxide growth. Werkstoffe und Korrosion 41, 383-390.

Mattsson, H., C. Li & I. Olefjord. 1990: Analysis of oxide formed on titanium during exposure in bentonite clay. II. The structure of the oxide. Werkstoffe und Korrosion 41, 578-584.

McGinnes, D. F. 2002: Model (reference) radionuclide inventory for reprocessing waste and spent fuel. Nagra NTB 01-01.

Mogensen, M., J.H. Pearce & C.T. Walker. 1999. Behaviour of fission gas in the rim region of high burn-up UO_2 fuel pellets with particular reference to the results from an XRF investigation. J. Nucl. Materials, 264, pp.99-112.

Nagra 1994: Kristallin-1 Safety Assessment Report, Nagra Technical Report NTB 93-22.

Neal, W.I., S.A. Rawson & W.M. Murphy. 1988: Radionuclide release behaviour of light water reactor spent fuel under hydrothermal conditions. Scientific Basis for Nuclear Waste Management XI, (M.J. Apted and R.E. Westerman, Editors), Mat.Res. Soc. Symp. Proc. 112, pp. 505-515.

Oversby, V.M. & H.F. Shaw. 1987: Spent fuel performance data: An analysis of data relevant to the NNWSI project. Lawrence Livermore National Laboratory Report UCID-20926.

Poinssot, C. P. Toulhoat, J-P. Grouiller, J. Pavageau, J-P. Piron, M. Pelletier, P. Dehaudt, C. Capellaere, R. Limon, L. Desgranges, C- Jegou, C. Corbel, S. Maillard, M-H. Fauré, J-C. Cicariello & M. Masson. 2001: Synthesis on the long-term behavior of the spent nuclear fuel. Volume 1. CEA Report CEA-R-5958(E), CEA Saclay.

Poinssot, unpublished data.

Rothman, A.J. 1984. Potential corrosion and degradation mechanisms of Zircaloy cladding on spent fuel in a tuff repository. Lawrence Livermore National Laboratory report UCID-20172.

Schrire, D., I. Matsson & B. Grapengiesser. 1997: Fission gas release in ABB SVEA 10x10 BWR fuel. Proc. Int. Top. Mtg. LWR Fuel Performance. 104-117, American Nuclear Society, La Grange Park. Ill.

Shoesmith, D.W. 2000. Fuel corrosion processes under waste disposal conditions. J. Nucl. Mats. 282, pp. 1-31.

SKB. 1999. SR 97. Processes in the repository evolution. SKB Technical Report TR-99-07.

Shoesmith, D.W. 2000. Fuel corrosion processes under waste disposal conditions, J. Nucl. Mat. 282, pp. 1-31.

Smith, H.D. & D.L. Baldwin. 1993: Thermal release of ^{14}C from PWR Zircaloy spent fuel cladding, J. Nucl. Mat. 200, 128-137.

Spahiu, K., Werme, L. & Eklund, U.-B. (2000): The influence of near field hydrogen on actinide solubilities and spent fuel leaching. Radiochim. Acta, 88/9-11, 507-511.

Spino, J. 1998: State of the technology review. In Advances in Fuel Pellet Technology for Improved Performance at High Burnup. IAEA-TECDOC-1036, Proc. of a Technical Committee Meeting, Tokyo, 28 Oct.- 1 Nov. 1996. IAEA, Vienna.

Stroes-Gascoyne, S., J.C. Tait, R.J. Porth, J.L. Mcconnell, T.R. Barnsdale & S. Watson. 1993: Measurement of grain-boundary inventories of ^{137}Cs, ^{90}Sr and ^{99}Tc in used CANDU fuel. In Mat. Res. Soc. Symp. Proc. 294, pp. 41-46.

Stroes-Gascoyne, S., J.C. Tait, R.J. Porth, J.L. Mcconnell, & W.J. Lincoln. 1994: Release of ^{14}C from the gap and grain-boundary regions of used CANDU fuels to aqueous solutions. Waste Management, 14, 385-392.

Stroes- Gascoyne, S., L.H. Johnson, J.C. Tait, J.L. McConnell & R.J. Porth. 1997. Mat. Res. Soc. Symp. Proc. 465, p. 511. et al.

Tait, J.C., R.J.J. Cornett, L.A. Chant, J. Jirovec, J. Mcconnell & D.L. Wilkin. 1997: Determination of Cl impurities and ^{36}Cl instant release from used CANDU fuels. In Scientific Basis for Nuclear Waste Management XX, (I. Triay and W.J. Gray, Editors), Mat. Res. Soc. Symp. Proc. Boston, USA, 1996. MRS, Pittsburgh, Pennsylvania.

Van Konynenburg, R.A., C.F. Smith, H.W. Culham & H.D. Smith. 1987: Carbon-14 in waste packages for spent fuel in a tuff repository. In Scientific Basis for Nuclear Waste Management X, (J.D. Bates and W.B. Seefeldt, Editors), Mat. Res. Soc. Symp. Proc. 84, pp.185-196.

Vesterlund, G. & L.V. Corsetti. 1994: Recent ABB fuel design and performance experience, Proc. of the 1994 International Topical Meeting on Light Water Reactor Fuel Performance, West Palm Beach, Florida, April 17-21, p.62, ANS.

Videm, K. 1981. Corrosion studies of candidate materials for permanent storage of nuclear waste. In Proc. Int. Congress on Metallic Corrosion, Mainz.

Wada, R., T. Nishimura, K. Fujiwara, M. Tanabe & M. Mihara. 1999. Experimental study on hydrogen gas generation rate from corrosion of Zircaloy and stainless steel under anaerobic alkaline condition, in Radioactive Waste Management and Environmental Remediation, In ICEM Conference Proceedings, Nagoya, Japan, Sept. 26-30, 1999, ASME.

Wegen, D., D. Papaioannou, J.-P. Glatz ,P.D.W. Bottomley, M. Amme & S. van Winckel, Post-leaching studies of defect rodlets. ICEM'03: The 9th International Conference on Environmental Remediation and Radioactive Waste Management,September 21 – 25, 2003, Examination Schools, Oxford, England.

Wilson, C.N. 1987: Results from Cycles 1 and 2 of NNWSI Series 2 Spent Fuel Dissolution Tests. HEDL-TME 85-22 UC-70, Westinghouse Hanford Company.

Wilson, C.N. 1990; Resultsfrom NNWSI Series 3 Spent Fuel Disolution Tests. PNL-7170, Pacific Northwest Laboratory, Richland , Washington.

Wilson, C.N. 1988: Summary of results from the series 2 and series 3 NNWSI bare fuel dissolution tests, in Scientific Basis for Nuclear Waste Management XI, (M.J. Apted and R.E. Westerman, Editors), Mat. Res. Soc. Symp. Proc. 112, p. 473.

Wilson, C.N. & W.J. Gray. 1990: Measurement of soluble nuclide dissolution rates from spent fuel. In Scientific Basis for Nuclear Waste Management XIII, Mat. Res. Soc. Symp. Proc. 176, pp. 489-498.

Wilson, C.N. & H.F. Shaw. 1987: Experimental study of the dissolution of spent fuel at 85 °C in natural groundwater. In Scientific Basis for Nuclear Waste Management X (J.D. Bates and W.B. Seefeldt, Editors), Mat. Res. Soc. Symp.Proc. 84, pp. 123-130.

Yamaguchi,I., S. Tanuma, I. Yasutomi, T. Nakayama, H. Tanabe, K. Katsurai, W. Kawamura, K. Maeda, H. Katao, & M. Saigusa. 1999: A study on chemical forms and migration behaviour of radionuclides in hull wastes. In ICEM '99 Conference Proceedings, Nagoya, Japan, Sept. 26-30, 1999, ASME.

Yokote, M., Y. Kondo, & S. Abeta, 1996: PWR fuel performance and burnup extension in Japan. Proc. 10th Pacific Basin Nuclear Conference, Kobe, Japan, 20-25 October, 1996.